Surface Properties Are Highly Sensitive to Small pH Induced Changes in the 3-D Structure of α-Lactalbumin†

Chunli Gao,‡ Ramani Wijesinha-Bettoni,§ Peter J. Wilde,‡ E. N. Clare Mills,‡ Lorna J. Smith,§ and Alan R. Mackie*,‡

Structuring Food for Health Programme, Institute of Food Research, Norwich Research Park, Colney NR4 7UA, U.K., and Inorganic Chemistry Laboratory, Department of Chemistry, University of Oxford, South Parks Road, Oxford OX1 3QR, U.K.

Received May 23, 2007; Revised Manuscript Received July 30, 2007

ABSTRACT: The change in structure of bovine α-lactalbumin in environments of decreasing pH from pH 7 to pH 3 was followed using high-resolution NMR and hydrogen exchange studies. The effect of the changes in the structure on the surface properties of the protein was also measured. As the pH was decreased from pH 7 toward pH 2, at which α-lactalbumin adopts a molten globule state, a small but increasing proportion of the molecules in the sample partially unfold. There was on average a loss of tertiary structure and a change in the environment of the tryptophan residues. A significant proportion of the change measured by both circular dichroism spectroscopy and interfacial methods observed as the pH was decreased from pH 7 to pH 4 was found to be irreversible upon readjustment back to pH 7. These changes in the sample conferred an increase in surface hydrophobicity and affected the surface properties. The surface activity was found to be highest at pH 4. This was because the increasing flexibility and surface hydrophobicity of the molecule with decreasing pH was balanced by the simultaneous increase in net charge repulsion. This conclusion was also confirmed by measurements of surface shear rheology. Interestingly the interfacial dilatational rheology was highest at the isoelectric point, indicating the dominant role of the charge interaction in controlling this parameter.

Lactose is the main source of carbohydrate in mammalian milk, and α-lactalbumin (αLA)[1] is an important milk protein involved in its biosynthesis through the interaction with lactose synthase. αLA is a globular calcium binding metalloprotein expressed exclusively during lactation. αLA constitutes roughly 20% of bovine whey (*1*), the remaining 80% being mostly *β*-lactoglobulin. As a result it is an important component of the food ingredients whey protein isolates (WPI) and concentrates (WPC). It has long been known that at low pH αLA forms a partially folded molten globule (MG) state in which the secondary structure is largely unaffected but most of the persistent tertiary structure is lost (*2*). Data from X-ray crystallography have provided a detailed structure of bovine αLa (*3*) and identified regions that are important for biological functionality and the likely impact of conformational stability of these regions. However, more recently the use of NMR has enabled structural studies to be undertaken looking at the effects of calcium binding and pH (*4*−*6*). These have shown the importance of long-range interactions in stabilizing the ensemble of conformations that is the MG state and the increased stability that is induced by the binding of Ca^{2+}. This stability is conferred primarily upon the C-helix of the α-domain and the 3_{10} helix in the *β*-sheet domain, which surround the Ca^{2+} binding site.

At neutral pH, αLa is in the native state and *β*-lactoglobulin dominates the surface properties of whey. However, at low pH (∼pH 2) αLA is in the MG state and plays an important role, even though it is the minor component. It has been shown that the loss of structure during the native to MG transition is associated with changes in surface properties. In particular the rate of adsorption to the air/water interface has been shown to be faster in the MG state despite the fact that the magnitude of the net charge on the molecule is much higher (*7*). This was attributed to a 15-fold increase in the surface hydrophobicity of the molecule in the MG state as opposed to the native state. This clearly significantly increased the residence time on the surface during the early stages of adsorption and was enough to overcome the increased intermolecular repulsion caused by the increased net charge at low pH (*7*). Interestingly the area occupied by the molecule when adsorbed to the interface at a certain surface pressure was found to be the same in both the native and MG states and different from the area obtained from the adsorption of fully denatured molecules. Although the rate and extent of adsorption were found to be higher in the MG state, the shear storage and loss moduli were found to be reduced. This information combined with FTIR data (*8*) lends credence to the idea that the adsorbed molecule is not in the MG state as had been suggested previously (*9*).

† This work was funded by the U.K. Biotechnology and Biological Sciences Research Council under joint Grants BBS/B/12393 (IFR) and BBS/B/12466 (University of Oxford).

* Author to whom correspondence should be addressed. Tel.: +44 (0)1603 255261, Fax: +44 (0)1603 507723, E-mail. alan.mackie@bbsrc.ac.uk.

‡ Norwich Research Park.

§ University of Oxford.

[1] Abbreviations: NMR, nuclear magnetic resonance; TOCSY, total correlation specroscopy; NOESY, nuclear Overhauser effect spectroscopy; COSY, $^1H-^1H$ correlation spectroscopy; CD, circular dichroism; FTIR, Fourier transform infrared; SEC, size exclusion chromatography; MG, molten globule; αLa, α-lactalbumin; WPC, whey protein concentrate; WPI whey protein isolate.

10.1021/bi700999r CCC: $40.75
Published on Web 01/18/2008

It is the decrease in stability imparted by the loss of fixed tertiary interactions that is responsible for the improved interaction of αLa with phospholipid vesicles at low pH (*10*, *11*). Thus in acidic environments such as that found in the gastric compartment, the partial penetration of the protein, into the alkyl region of the lipid vesicles limits access of proteolytic enzymes. This has a limiting effect on hydrolysis and means that the protein is likely to remain intact until it has entered the small intestine and may be more likely to be presented to the immune system in an intact form. Much work has been undertaken looking at the significance of this interaction (*12*, *13*) including the effect of the protein lipid vesicle interaction on proteolysis during simulated gastric digestion (*14*). While electrostatic and hydrophobic interactions are undoubtedly important, a certain molecular flexibility is also thought to be required (*15*). The interaction with lipid vesicles is anchored by the A and C helices (*16*). Vesicle curvature is also thought to play a role. The loss of persistent tertiary structure is probably also responsible for the improvement in surface functionality at low pH (*9*). Understanding the conformational changes in the protein which are responsible for controlling adsorption, unfolding, and interaction at the interface are vital if we are to fully comprehend the biological activity of αLa and obtain a more molecular description of the behavior of proteins at interfaces. In this initial study, we have used a combination of high-resolution NMR and interfacial techniques such as pendant drop and surface dilatational and shear rheology in an attempt to identify the structural changes responsible for the interfacial properties of αLA as a function of pH.

EXPERIMENTAL PROCEDURES

1. Protein Samples. Purified bovine αLA (type I) and all other reagents were purchased from Sigma Chemical Co., St Louis, MO, and used without further purification.

2. Sample Solution Preparation. Solutions of αLA (0.1 mM) were prepared with 0.1 M, pH 7 sodium citrate buffer containing 0.2 mM $CaCl_2$. A range of lower pH solutions was prepared in duplicate by the addition of 0.1 M citric acid. The pH 4 sample was then readjusted back to pH 7 with 0.2 M NaOH. Samples were equilibrated at 4 °C overnight before analysis and diluted to appropriate concentrations with deionized water (NANOpure DIamond, Barnstead, Dubuque, IA). The final protein and calcium concentrations were maintained for all samples during pH adjustment.

3. Interfacial Measurements. The surface tension (γ) and surface dilatational elastic modulus (E') were measured using an FTA200 pulsating drop tensiometer (First Ten Ångstroms, Portsmouth, VA). The method measures the surface tension using the pendant drop technique in which an image of a liquid droplet hanging from the tip of a syringe is captured. The shape of the drop (determined by its density and the surface tension) is analyzed using a derivation of the Young−Laplace equation (equation of capillarity) to give the surface tension. The surface dilatational modulus is calculated from the response of the surface tension to changes in surface area (A) caused by the drop volume being oscillated sinusoidally using a computer controlled pump. The interfacial dilatational modulus E is given by $E = d\gamma/d \ln A$, where $d\gamma$ is the change in surface tension resulting from the relative change in surface area $d \ln A (= dA/A)$. The frequency and amplitude of the resultant sine waves were analyzed using fast Fourier transform analysis to produce mean values of $d\gamma$ and dA over a specified time period. The initial drop volume was 12 μL, the applied surface area oscillations had a relative amplitude of 5% to avoid excessive perturbation of the interfacial layer, and the measurement frequency was 0.05 Hz. All measurements were made at room temperature. Surface shear rheology was measured using a Camtel CIR-100 interfacial shear rheometer (Camtel Ltd., Royston, U.K.). The measurement was carried out as described previously (*17*).

4. Circular Dichroism Measurements. Far-UV (190−260 nm) and near-UV (250−350 nm) circular dichroism (CD) spectra were recorded at 20 °C using a J-710 CD spectra polarimeter (Jasco Ltd., Tokyo, Japan) using 0.5 and 10 mm path length cells, respectively. Spectra were collected on the average of four accumulations at 100 nm/min, with a 2 s time constant, 0.5 nm resolution, and sensitivity of ±100 mdeg. All data were calculated in terms of molar elipticity, which is the raw data normalized for path length and molar concentration.

5. Fluorescence Spectroscopy. Fluorescence measurements were performed at 20 °C with a LS 55 luminescence spectrometer (Perkin-Elmer, Wellesley, MA) using a quartz cuvette with 1.0 cm path length. The fluorescence spectra were collected in the 300−400 nm range with excitation at 280 nm using excitation and emission slits at 5 nm; the scan speed was 100 nm/min.

6. NMR Spectroscopy. The samples were prepared in 95/5 H_2O/D_2O and 2.8 mM $CaCl_2$ at a protein concentration of 1.2 mM. NMR experiments were carried out on home-built spectrometers at the Oxford Centre for Molecular Sciences, at 500, 600, or 750 MHz. One-dimensional spectra were collected at pH 2, 3.5, 4, 5, and 7 at 25 °C. In addition, a 1D spectrum was collected of a sample which was initially prepared at pH 3.5, left overnight at pH 3.5, and then adjusted to pH 7, together with a sample prepared directly at pH 7, both collected at 30 °C. The pH 5 solution resulted in some protein precipitation by the end of data collection. The data were collected and processed as described by ref *18*.

7. Hydrogen-Exchange Experiments. **A** 1.2 mM amount of αLA in 2.8 mM $CaCl_2$ (H_2O) was freeze-dried at the required pH values and redissolved in deuterated buffer to initiate H-exchange. A 50 mM amount of deuterated imidazole buffer was used at pH 7, while 25 mM deuterated sodium acetate buffer was used for pH 3.5, 4, and 5, to ensure that the sample dissolved at the required pH. The data were collected and processed as described by ref *18*. Hydrogen exchange rates were determined and protection factors obtained as described in ref *18*. For the NHs where the decay in intensity is insufficient during the time course of the experiment to obtain rates by curve fitting, k_{int} was taken as 10^{-4} min^{-1} in order to estimate the lower limits of the protection factors. For the NHs that exchanged too fast (and therefore did not have enough data points to fit the decay function) an estimate (*19*) of the experimental rates has been used to obtain the protection factors. Hydrogen exchange in the molten globule state was initiated by dissolving 200 mg of lyophilized protein in 11 mL of D_2O at pH 2 at 25 °C. Aliquots of 1.1 mL each (protein concentration, 1.28 mM) were removed, after exchanging for various lengths of time ranging from 1 min to 3.5 h. Immediately prior to quenching

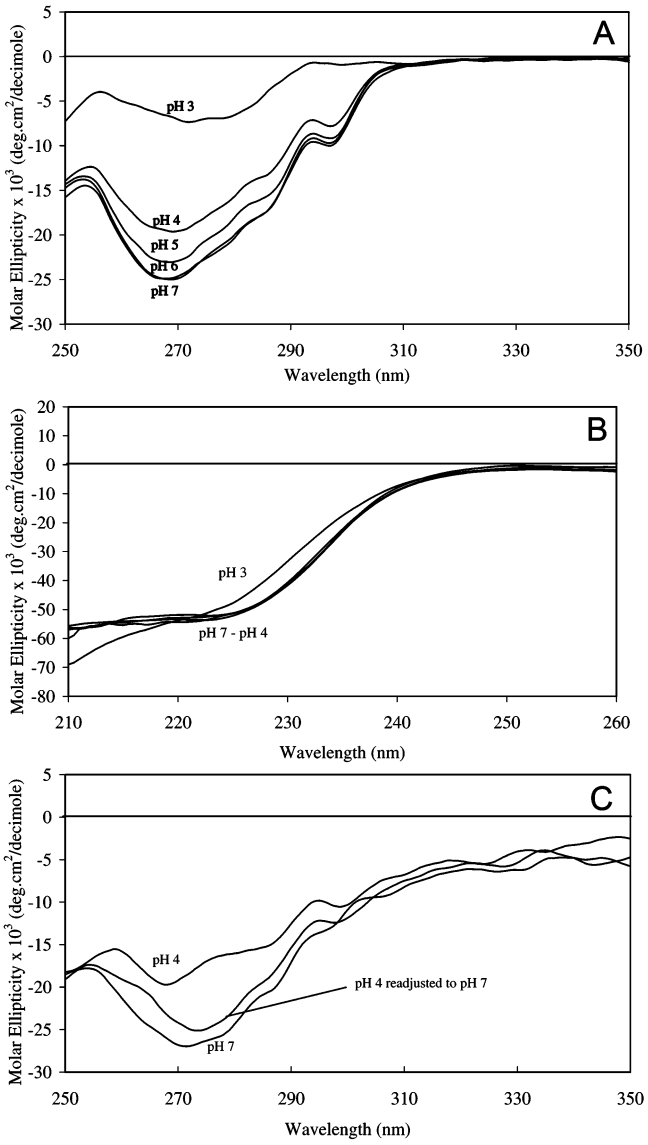

FIGURE 1: CD spectra (molar elipticity) of αLA measured at different pH: (A) near-UV; (B) far-UV. 0.05 mM αLA in 0.05 M citrate buffer containing 0.1 mM $CaCl_2$; (C) near-UV CD spectrum of 4 μM αLA in 0.4 mM citrate buffer containing 8 μM $CaCl_2$.

(by immersing in liquid N_2), 2.8 mM $CaCl_2$ was added and the samples were lyophilized. The samples were then redissolved at pH 5.5 in 100 mM sodium acetate buffer. Some of the time points were repeated from a different batch of protein to test reproducibility. Phase sensitive COSY spectra (*20*) were acquired at 30 °C in order to identify the protected amide hydrogens. Hydrogen exchange rates were monitored by measuring peak heights in the COSY spectra. These were normalized relative to the intensities of the nonexchangeable aromatic protons, as reported in literature (*21*). These data were fitted to a single-exponential decay and the protection factors calculated in the same manner as described above for the native state (*22*).

RESULTS AND DISCUSSION

1. pH Denaturation of αLA. While the near-UV CD spectra (Figure 1A) showed no change in tertiary structure of αLA between pH 7 and pH 6, a gradual decrease in persistent tertiary structure was observed as the pH decreased

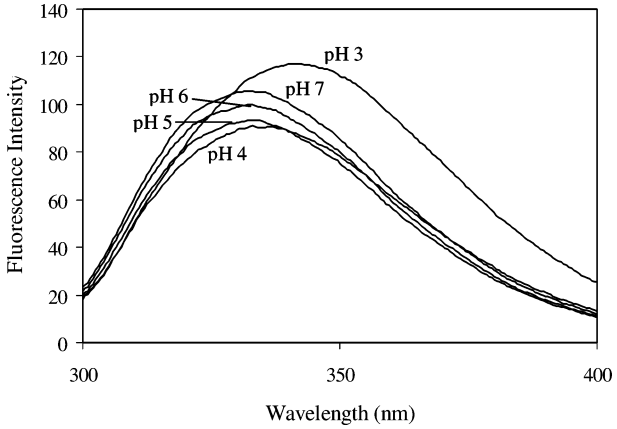

FIGURE 2: Fluorescence emission spectra of αLA at different pH. Samples contained 0.5 μM αLA in 0.5 mM citrate buffer containing 1.0 μM $CaCl_2$.

below 6. The far-UV spectra (Figure 1B) indicated no major secondary structural changes from pH 7 to pH 4, although the signal was reduced at 230 nm and increased at 210 nm in the sample at pH 3. This result is consistent with what has been seen by others (*23*) who have shown that the MG transition corresponds to a loss of fixed tertiary interactions and that the α-helical domain in the molecule is highly stable to changes in pH.

The α-La molecule has four tryptophan (W) residues at positions W26 in the B-helix, W60 in the β-domain, W104 in the D-helix, and W118 in aromatic cluster 1. We have made use of these to probe changes in conformation by measuring the intrinsic fluorescence. The spectra (Figure 2) showed the emission maximum red-shifted slightly (2 nm) at pH 4 and more significantly (10 nm) at pH 3 where the intensity also increased. These changes show that on average the tryptophan residues were experiencing a more polar environment as the pH decreased below 5, and therefore were more likely to make the surface of the molecule more hydrophobic.

The structural changes induced by varying pH were also investigated using high-resolution 1D-NMR (Figure 3). The spectrum of the native *holo* state of αLA at pH 7 (Figure 3A) shows sharp resonance signals and a large chemical shift dispersion, reflecting highly specific interresidue interactions within a single unique conformation with only small fluctuations about the average folded structure. At pH 5, a similar spectrum was observed. The 1D NMR spectra at pH 4 and 3.5 show large chemical shift dispersion, but the resonances are fairly broad when compared to the spectrum at pH 7. Such line broadening could be caused by aggregation, as higher molecular weight species tumble more slowly. However, the αLa remained monomeric as determined by SEC. The line broadening is therefore likely to reflect intermediate time-scale motions occurring within at least a fraction of the protein molecules in the sample. The spectrum at pH 2 (Figure 3E) was that of the MG state and shows characteristic marked broadening of the resonance lines. This field-dependent line broadening is typical of intermediate exchange processes and is consistent with interconversion among a number of different conformations within the MG ensemble on a millisecond time scale (*24*, *25*). The MG is somewhat expanded when compared to the native state and

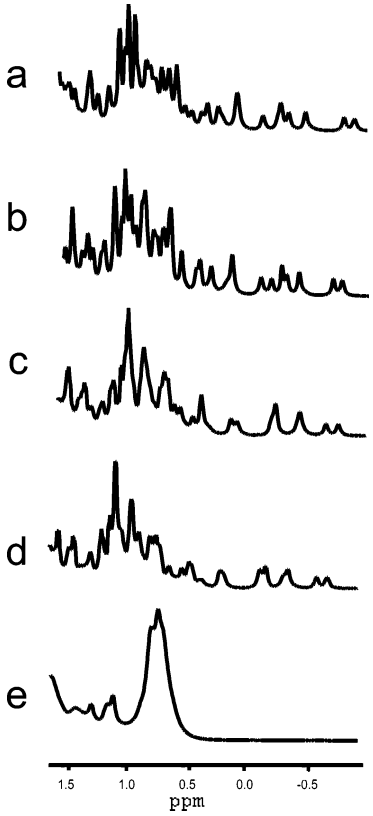

FIGURE 3: Upfield region of NMR spectra of BLA samples in 95/5 H_2O/D_2O at (A) pH 7, (B) 5, (C) 4, (D) 3.5, and (E) 2. All measurements were acquired at 25 °C.

is highly heterogeneous. Also, the chemical shift dispersion is significantly reduced, and the chemical shifts of many resonances are close to random coil values.

To describe these changes in more detail, the 2D TOCSY and NOESY spectra at the various pH values were inspected. At the higher pH values, the spectra showed only typical native signals, confirming that the greater part of the sample retains the native structure. The pH 2 MG spectrum showed mainly a few very broad resonances. The 2D NMR spectra were assigned at the various pH values, by comparison with published assignments (*26*), although it was not possible to assign all residues at all the pH values studied. As in previous work with αLA (*26*, *27*) we found that the B-helix and D-helix gave very broad peaks that were difficult to assign, due to the changes in the ionization state of H32 and H107.

A comparison of the NH and Hα chemical shifts of αLA at pH 7 and the other pH values studied was carried out. These data are available as Supporting Information. Most values for NH were similar between the pH 7 and pH 5 data, with only two residues showing a difference larger than ±0.2 ppm. Between pH 7 and pH 4 data, five residues showed a difference greater than ±0.2 ppm, and between pH 7 and pH 3.5 data, four residues. The values for Hα chemical shifts varied even less, with only a few residues showing a difference larger than ±0.1 ppm. To see if the observed chemical shift differences were due to changes in protonation states of Asp, Glu, and His residues, the PDB coordinates for αLA (1HFZ) were analyzed. The analysis concentrated on Asp, Glu, and His residues as it is very likely that their side chains will change protonation state over the pH range studied. In particular, residues whose NH and Hα atoms were closer than 5 Å to the OE1/OE2 protons of Glu, the OD1/OD2 protons of Asp, or the ND1 proton of His residues were identified. We also considered residues that were adjacent in sequence to Glu, Asp, or His. All the sizable difference between chemical shifts at the various pHs studied were associated with these residues that are close to Asp, Glu, or His side chains. Thus, these changes can be attributed to differences in electrostatic interactions rather than arising from structural changes over the pH range studied here. These data are available as electronic Supporting Information. However, we note that only partial information is available regarding residues in the B-helix and D-helices from the chemical shift data, due to the incomplete resonance assignments for these regions of the sequence, as discussed previously.

The analysis of chemical shifts observed in the spectra recorded for αLA at different pH conditions gives no evidence for significant change to the native state structure of the protein as the pH is decreased. The line broadening effects observed in the spectra are therefore most likely to reflect the fact that in the sample there is equilibrium between protein molecules in the native and molten globule states. The native state predominates, and these are the molecules whose resonances are observed in the NMR spectra. The fraction of molecules in the molten globule state is small but increases as the pH is lowered. This partial unfolding of a fraction of the molecules could lead to the observed changes in the CD and fluorescence spectra as these techniques probe an average over the full conformational ensemble populated.

Hydrogen exchange is a powerful tool for probing a protein's conformational stability (*28*). Figure 4 summarizes the hydrogen exchange results for *holo* αLA at the various pH values studied, while Figure 5 shows where the residues with protected backbone amide groups are located in the 3D structure. All experiments were undertaken in the presence of Ca^{2+} to avoid the *apo* form affecting hydrogen exchange. The intrinsic rate of hydrogen exchange (k_{int}) will increase with the increase in pH on going from pH 2 to pH 7 (*29*). The hydrogen exchange will be fastest at pH 7 with a 10-fold decrease in rate expected for a one unit pH decrease (*30*). The data in Figure 4 show that the patterns of hydrogen exchange protection at pH 7 and 5 are similar, although the values of the protection factors are on average larger at pH 7, suggesting there is slightly more protection. However, a higher number of residues show some level of hydrogen exchange protection at pH 5 (43 NHs) than at pH 7 (34 NHs). As most of these protected residues have rather low protection factors, they may reflect the lower k_{int} at pH 5 compared with pH 7. There is a substantial decrease in the protection factors at pH 4, with less residues (26 NHs) showing some level of hydrogen exchange protection. There is a sizable change in the protection factor of W60 between pH 4 and pH 5, suggesting that this is the main tryptophan residue responsible for the differences in intrinsic fluorescence seen between pH 4 and pH 5 (Figure 2). The data at pH 3.5 show approximately the same number of protected amides when compared to pH 4. Under the two conditions there are some differences in which residues have protected backbone amide groups. However, the protection factors are significantly smaller at pH 3.5 than at pH 4. The pattern of hydrogen exchange protection observed at pH 3.5 (Figure 4) is similar to that seen in the pH 2 molten globule state, with the C-helix

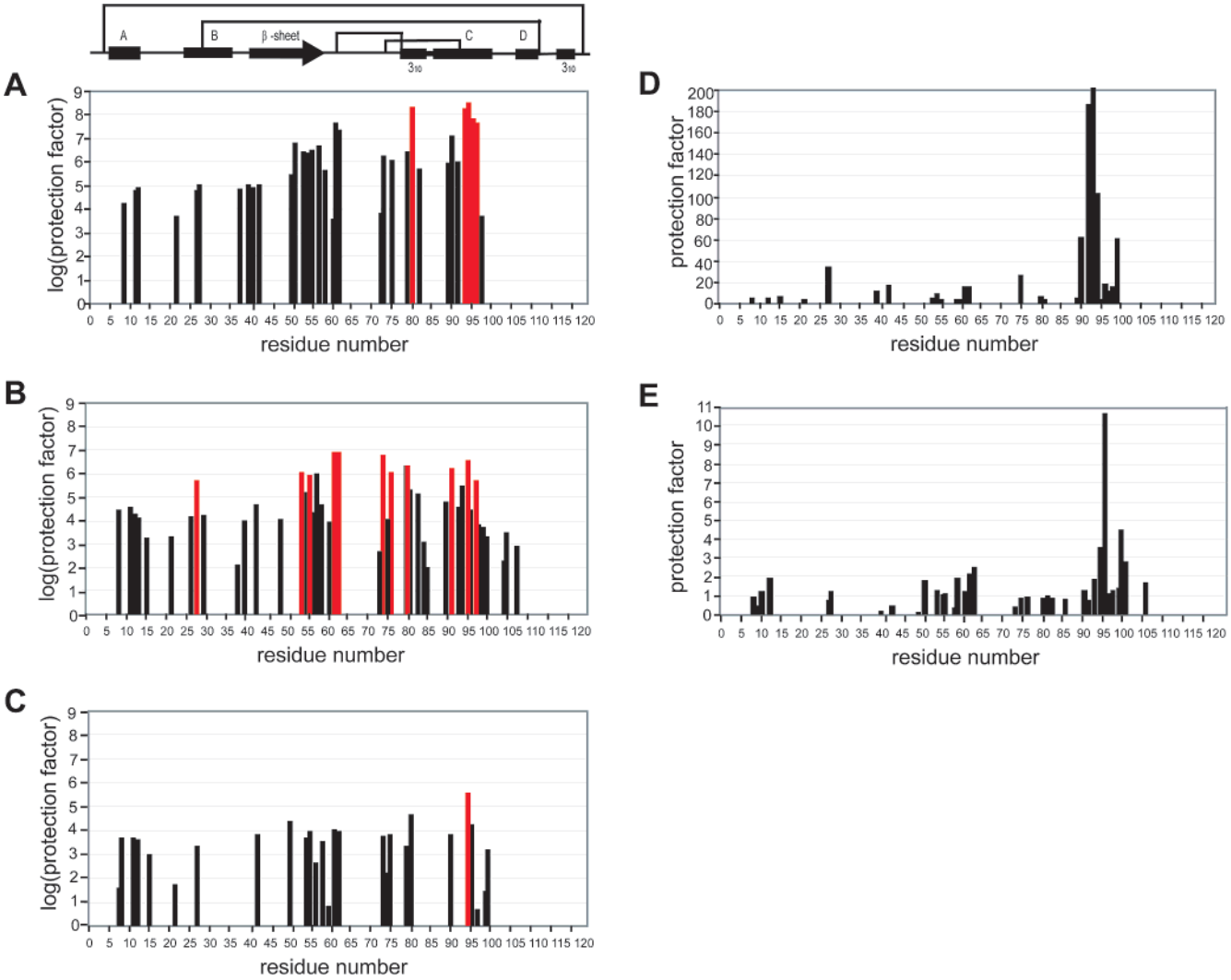

FIGURE 4: Histograms showing the distribution of protection factors for backbone amide hydrogen exchange for (A) pH 7, (B) 5, (C) 4, (D) 3.5, and (E) p2, at 25 °C. The pH 2 molten globule data have been obtained from "pH jump" experiments, where hydrogen exchange occurs at pH 2 and is quenched by jumping to native conditions, followed by acquisition of the spectrum. The protection factors are plotted on a logarithmic scale (log) as a function of residue number for A−C, while the actual values are plotted in D and E. The positions of the regions of secondary structure found in the native structure (labeled A−D for the α-helices, 3_{10} for the 3_{10} helices, and β-sheet) and the disulfide bridges are shown schematically above the plots. Red bars correspond to NHs that exchange too slowly during the time course of the experiment for their rates to be measured. For these residues the values shown are the lower limits of the protection factors. The protection factor for V92 in D is 258.

showing a marginally higher level of hydrogen exchange protection than the rest of the protein. Nevertheless, the 1D NMR data (Figure 3) show that the protein at pH 3.5 is, on average, very different from the molten globule state. The hydrogen exchange data support the hypothesis that as the pH decreases a small but increasing proportion of the molecules partially unfold into a state that is molten globule-like. Published studies (*28*) on αLA show that the thermal denaturation of αLA to the MG state is dependent on temperature and pH, with the denaturation temperature (T_d) at pH 3.5, 4.2, 5.2, and 8.0 being, respectively, 41, 56.9, 63, and 68.3 °C. Even though the present hydrogen exchange study has been done at 25 °C, it seems likely that at pH 3.5 a small fraction of the protein does remain in the molten globule state, with an even smaller fraction at pH 4.

All of the methods applied to determine structural changes induced by reducing pH show they are dominated by an increase in polypeptide flexibility for at least a fraction of the molecules present in the sample. This is reflected by the loss of tertiary structure which is accompanied by specific changes in the β-domain of the protein. As the pH was reduced, both the extent of structural changes and the proportion of αLA affected increased, although the structure of the major constituent of the protein at pH 3.5 is still nativelike, while the differences between pH 7 and pH 5 were minimal.

2. Surface Properties. The impact of the pH induced structural changes on the surface activity of αLA was then investigated. The results (Figure 6a) are shown in terms of surface pressure (surface tension of buffer − surface tension of sample) as a function of time over 17 min for 4 μM solutions of αLA at different values of pH. The surface activity was lowest at neutral pH, when the protein was in the "native" conformation, and then gradually increased as the pH decreased, reaching a maximum at pH 4. The surface pressure data for pH 3 and 5 are very similar even though the NMR data suggest that the there would have been a proportion of molecules in a MG-like state at pH 3. The

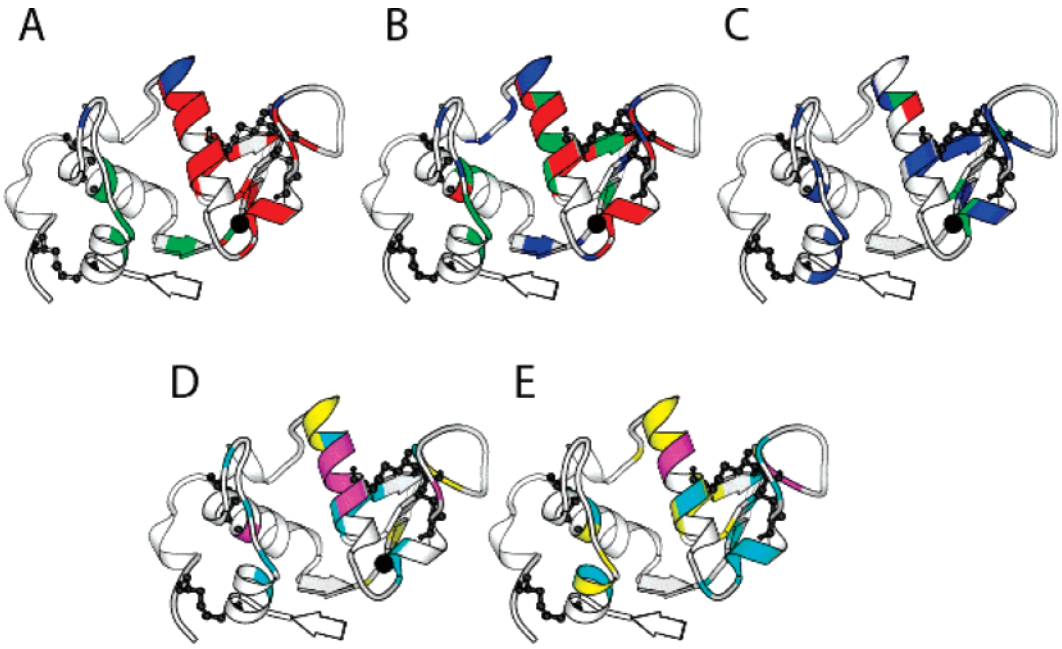

FIGURE 5: Regions that have significant hydrogen exchange protection in BLA, at (A) pH 7, (B) 5, (C) 4, (D) 3.5, and (E) 2 on the 3D structure of α-lactalbumin. In A−C, residues with a protection factor log < 4 are colored blue, log between 4 and 5 green, and >5 in red. In D, cyan corresponds to a protection factor <10; yellow, between 10 and 20; and magenta, >20. In E, cyan corresponds to a protection factor <1; yellow, between 1 and 2; and magenta, >2.

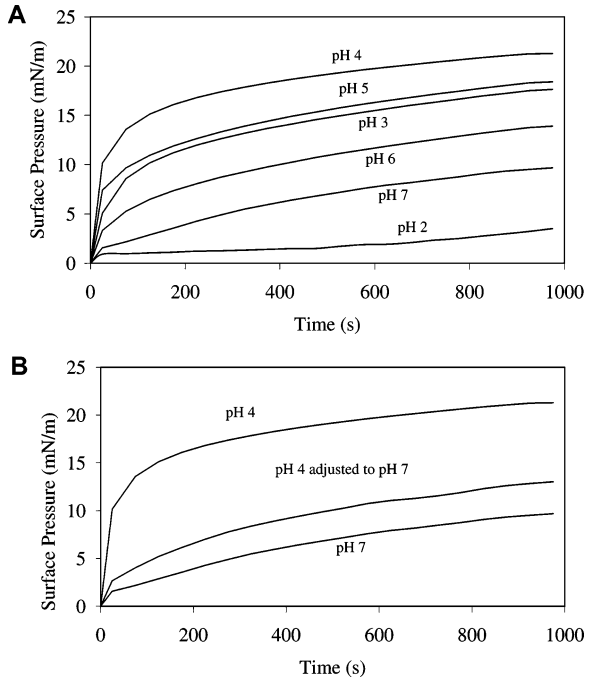

FIGURE 6: Surface pressure as a function of adsorption time at different pH, 4 μM αLA in 0.4 mM citrate buffer containing 8 μM $CaCl_2$ at fixed pH (A) and after cycling between pH 4 and pH 7 (B).

likely cause of this discrepancy is that there are two competing factors that influence the rate of adsorption and thus the rate at which the surface tension is decreased. The first factor is the flexibility of the adsorbing protein molecule, which is clearly influenced by the amount of protein in the molten globule conformation. The more flexible the molecule is, the more rapidly it can adopt a conformation suitable for adsorption to the interface. It has also been shown that the surface hydrophobicity of the molecule is much greater (15-fold) in the molten globule state (*7*). This would also affect the rate of exchange between the bulk phase and the interface, leading to an increase in residence time at the surface and thus a faster formation of an interfacial layer.

Table 1: Net Charge of αLa as a Function of pH

pH	charge	pH	charge	pH	charge
3.0	9.6	4.93	0.0	6.0	−2.6
4.0	4.1	5.0	−0.3	7.0	−4.5

The second factor affecting surface activity is the net charge on the molecule, which discourages the formation of a compact adsorbed layer due to the charge repulsion. Thus, the optimum pH for adsorption falls between the isoelectric point of the protein (pH 4.93) and the pH where the majority of molecules are in the most unfolded state. Calculation of the net molecular charge as a function of pH (Table 1) indicates that in fact the charge repulsion becomes much more dominant below the isoelectric point, with a net charge on the molecule of 9.6 at pH 3. Thus, if the net charge was the controlling parameter in determining interfacial tension, one would expect that αLA would be less surface active at pH 3 than at pH 7. However, it is more surface active at pH 3 than at pH 6 where the net charge is only −2.6. Thus, it is clear that the degree of unfolding, at least in terms of increasing polypeptide flexibility and loss of tertiary structure together with the resulting increase in surface hydrophobicity has a major influence on surface activity. These data highlight the importance of the transition to the MG state in improving the interfacial properties of αLA.

Further evidence for this conclusion is provided by the data for the interfacial dilatational elastic modulus shown in Figure 7. The interfacial rheology was plotted as a function of surface pressure as it is linked to the surface concentration and thus normalizes for differences in rates of adsorption.

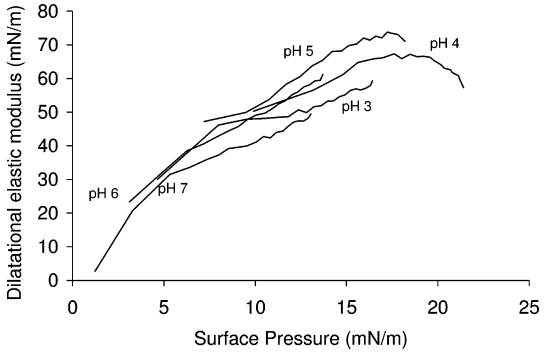

FIGURE 7: Surface dilatational modulus plotted as a function of the surface pressure for the same solutions as shown in Figure 1A,B.

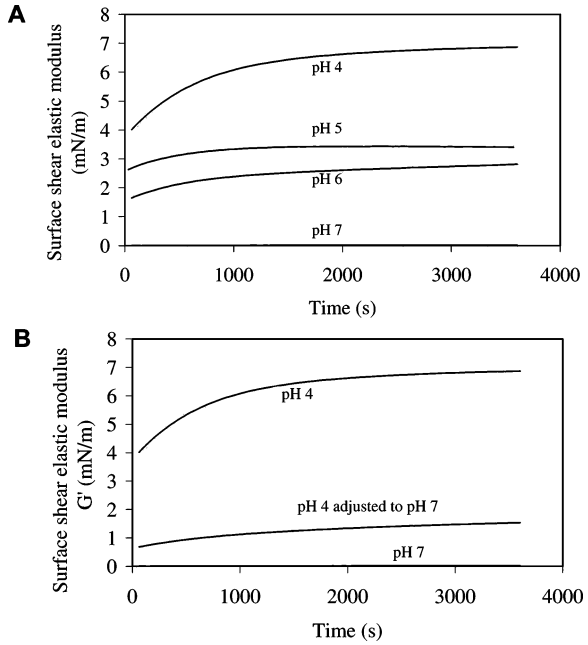

FIGURE 8: Surface shear elastic modulus (G') as a function of adsorption time at different pH for 2 μM αLA in 0.2 mM citrate buffer containing 8 μM $CaCl_2$ at fixed pH (A) and after cycling between pH 4 and pH 7 (B).

The figure shows the storage (elastic) part of the modulus and is an indication of the structural rigidity of the interfacial film in a regime of compressive (or expansive) perturbation. This is generally considered to be a measure of intramolecular interactions and stability. The data clearly show that the greatest elasticity was observed at pH 5, which is very close to the isoelectric point of αLA. This indicates that the most rigidly packed system was achieved at the lowest net charge regardless of the conformation of the molecule in solution. This is because the decrease in polypeptide stability affects the rates of adsorption and thus rates of increase in surface pressure rather than the final packing density that controls the dilatational rheology.

The intermolecular interactions in the interfacial film were also investigated as a function of pH through measurements of the interfacial shear rheology. Figure 8a shows the shear elastic modulus of 2 μM solutions of αLA measured over a period of 1 h. At pH 7 insufficient protein adsorbed to the interface to provide measurable shear rheology, but as the pH was decreased the shear elastic modulus increased, particularly at pH 4. This is in contrast to the dilatational data which were highest at pH 5 and show that conformation and surface hydrophobicity are important for the formation of intermolecular interactions, regardless of long-range electrostatic effects.

3. αLA Structure and Surface Properties When the pH Is Adjusted from pH 4 to pH 7. Figure 6B shows the increase in surface pressure of a 4 μM solution of αLA as a function of time. The data show the effect of readjusting the pH from 4 to 7 and is compared with the control samples maintained at pH 7 and 4. The pH adjusted sample shows a greater surface activity than αLA maintained at pH 7, indicating that there was an irreversible change in the αLA sample taken through a cycle of reducing the pH to 4 and readjusting to pH 7. Replicates of this experiment consistently showed the same behavior with final values of surface tension similar to better than 3%. The effect of pH adjustment from 4 to 7 on the surface shear elasticity of αLA (Figure 8B) shows that the pH adjusted sample forms a stronger interface than the control sample at pH 7. Both far- and near-UV CD spectroscopy of the pH adjusted sample (Figure 1) confirmed that a proportion of the αLA underwent an irreversible loss of tertiary structure at pH 4. Given that the charge on the molecule remains unchanged, the surface property analysis suggests that a significant proportion of either the structural change important for increased surface activity or the proportion of αLA molecules altered induced at pH 4 is retained upon readjusting the pH to 7. Only a limited irreversible component remained which increased the surface activity and surface shear modulus of the protein compared to its original state. The proportion of irreversibly altered αLA was too small to be observed by NMR spectroscopy.

CONCLUSIONS

In this paper we have linked the structural changes that αLA undergoes as a function of decreasing pH with the surface properties that these changes impart. As the pH decreases from 7 to 3, a proportion of the protein goes from its native conformation toward the molten globule conformation normally seen at pH 2. At the same time the net charge on the protein increases from −4.5 to +9.6, going through its isoelectric point at pH 4.93. Both the unfolding and the net charge have a marked effect on the surface properties of the protein. Above the isoelectric point the behavior is largely dominated by the net charge on the molecule so that the surface activity increases with decreasing pH. This is because the surface packing is affected by the charge density. However, below the isoelectric point when the charge density increases significantly with decreasing pH, the degree of unfolding and the surface hydrophobicity becomes much more important. Thus, the maximum values in surface pressure and shear modulus are reached at pH 4, where the magnitude of the net charge is nearly as high as at pH 7.

The results from the NMR experiments all point to the fact that there is minimal unfolding going from pH 7− to pH 5 but that, as the pH decreases below 5, the proportion of protein in the MG state increases. Further biophysical experiments in which the pH was readjusted from pH 4 to pH 7 showed that a small proportion of those molecules that had undergone a change in conformation at pH 4 did so irreversibly. Moreover approximately 25% of the conformational change responsible for the enhanced surface properties was irreversible.

SUPPORTING INFORMATION AVAILABLE

Figure showing a comparison of the NH and Hα chemical shifts of αLA at pH 7, 5, 4, and 3.5. This material is available free of charge via the Internet at http://pubs.acs.org.

REFERENCES

1. de Wit, J. N. (1998) Nutritional and functional characteristics of whey proteins in food products, *J. Dairy Sci. 81*, 597−608.
2. Wong, D. W. S., Camirand, W. M., and Pavlath, A. E. (1996) Structures and functionalities of milk proteins, *Crit. Rev. Food Sci. Nutr. 36*, 807−844.
3. Pike, A. C. W., Brew, K., and Acharya, K. R. (1996) Crystal structures of guinea-pig, goat and bovine alpha-lactalbumin highlight the enhanced conformational flexibility of regions that are significant for its action in lactose synthase, *Structure 4*, 691−703.
4. Quezada, C. M., Schulman, B. A., Froggatt, J. J., Dobson, C. M., and Redfield, C. (2004) Local and global cooperativity in the human alpha-lactalbumin molten globule, *J. Mol. Biol. 338*, 149−158.
5. Wijesinha-Bettoni, R., Dobson, C. M., and Redfield, C. (2001) Comparison of the structural and dynamical properties of holo and apo bovine alpha-lactalbumin by NMR spectroscopy, *J. Mol. Biol. 307*, 885−898.
6. Wirmer, J., Berk, H., Ugolini, R., Redfield, C., and Schwalbe, H. (2006) Characterization of the unfolded state of bovine alpha-lactalbumin and comparison with unfolded states of homologous proteins, *Protein Sci. 15*, 1397−1407.
7. Cornec, M., Kim, D. A., and Narsimhan, G. (2001) Adsorption dynamics and interfacial properties of alpha-lactalbumin in native and molten globule state conformation at air-water interface, *Food Hydrocolloids 15*, 303−313.
8. Dalgleish, D. G., and Fang, Y. (1998) Conformational aspects of α-lactalbumin as a function of pH, heat treatment and adsorption at hydrophobic surfaces studied by FTIR, *Food Hydrocolloids 12*, 121−126.
9. Matsumura, Y., Mitsui, S., Dickinson, E., and Mori, T. (1994) Competitive adsorption of alpha-lactalbumin in the molten globule state, *Food Hydrocolloids 8*, 555−566.
10. Chenal, A., Vernier, G., Savarin, P., Bushmarina, N. A., Geze, A., Guillain, F., Gillet, D., and Forge, V. (2005) Conformational states and thermodynamics of alpha-lactalbumin bound to membranes: A case study of the effects of pH, calcium, lipid membrane curvature and charge, *J. Mol. Biol. 349*, 890−905.
11. Hanssens, I., van Ceunebroeck, J. C., Pottel, H., Preaux, G., and Van Cauwelaert, F. (1985) Influence of the protein conformation on the interaction between alpha-lactalbumin and dimyristoylphosphatidylcholine vesicles, *Biochim. Biophys. Acta 817*, 154−164.
12. Agasoster, A. V., Halskau, O., Fuglebakk, E., Froystein, N. A., Muga, A., Holmsen, H., and Martinez, A. (2003) The interaction of peripheral proteins and membranes studied with alpha-lactalbumin and phospholipid bilayers of various compositions, *J. Biol. Chem. 278*, 21790−21797.
13. Berliner, L. J., and Koga, K. (1987) Alpha-lactalbumin binding to membranes: Evidence for a partially buried protein, *Biochemistry 26*, 3006−3009.
14. Moreno, F. J., Mackie, A. R., and Mills, E. N. C. (2005) Phospholipid interactions protect the milk allergen alpha-lactalbumin from proteolysis during in vitro digestion, *J. Agric. Food Chem. 53*, 9810−9816.
15. Banuelos, S., and Muga, A. (1996) Structural requirements for the association of native and partially folded conformations of alpha-lactalbumin with model membranes, *Biochemistry 35*, 3892−3898.
16. Halskau, O., Froystein, N. A., Muga, A., and Martinez, A. (2002) The membrane-bound conformation of alpha-lactalbumin studied by NMR-monitored H-1 exchange, *J. Mol. Biol. 321*, 99−110.
17. Ridout, M. J., Mackie, A. R., and Wilde, P. J. (2004) Rheology of mixed β-casein/β-lactoglobulin films at the air−water interface, *J. Agric. Food Chem. 52*, 3930−3937.
18. Wijesinha-Bettoni, R., Gao, C., Jenkins, J. A., Mackie, A. R., Wilde, P. J., Mills, E. N. C., and Smith, L. J. (2007) Heat treatment of bovine-lactalbumin results in partially folded, disulfide bond shuffled states with enhanced surface activity, *Biochemistry*, in press.
19. Wagner, G., and Wuthrich, K. (1982) Amide protein exchange and surface conformation of the basic pancreatic trypsin inhibitor in solution. Studies with two-dimensional nuclear magnetic resonance, *J. Mol. Biol. 160*, 343−361.
20. Bax, A., Freeman, R., and Frenkiel, T. A. (1981) An NMR technique for tracing out the carbon skeleton of an organic molecule, *J. Am. Chem. Soc. 103*, 2102−2104.
21. Chyan, C. L., Wormald, C., Dobson, C. M., Evans, P. A., and Baum, J. (1993) Structure and stability of the molten globule state of guinea-pig alpha-lactalbumin: a hydrogen exchange study, *Biochemistry 32*, 5681−5691.
22. Wijesinha-Bettoni, R. (2000) *Nuclear Magnetic Resonance Spectroscopic Studies of Bovine α-Lactalbumin in Solution*, University of Oxford, Oxford, U.K..
23. Kuwajima, K., Mitani, M., and Sugai, S. (1989) Characterization of the critical state in protein folding-Effects of guanidine-hydrochloride and specific Ca^{2+} binding on the folding kinetics of alpha-lactalbumin, *J. Mol. Biol. 206*, 547−561.
24. Baum, J., Dobson, C. M., Evans, P. A., and Hanley, C. (1989) Characterization of a partly folded protein by NMR methods: Studies on the molten globule state of guinea-pig alpha-lactalbumin, *Biochemistry 28*, 7−13.
25. Schulman, B. A., Redfield, C., Peng, Z. Y., Dobson, C. M., and Kim, P. S. (1995) Different subdomains are most protected from hydrogen-exchange in the molten globule and native states of human alpha-Llactalbumin, *J. Mol. Biol. 253*, 651−657.
26. Forge, V., Wijesinha, R. T., Balbach, J., Brew, K., Robinson, C. V., Redfield, C., and Dobson, C. M. (1999) Rapid collapse and slow structural reorganisation during the refolding of bovine alpha-lactalbumin, *J. Mol. Biol. 288*, 673−688.
27. Kim, S., and Baum, J. (1998) Electrostatic interactions in the acid denaturation of alpha-lactalbumin determined by NMR, *Protein Sci. 7*, 1930−1938.
28. Dempsey, C. E. (2001) Hydrogen exchange in peptides and proteins using NMR spectroscopy, *Prog. Nucl. Magn. Reson. Spectrosc. 39*, 139−170.
29. Bai, Y. W., Milne, J. S., Mayne, L., and Englander, S. W. (1993) Primary structure effects on peptide group hydrogen exchange, *Proteins: Struct., Funct., Genet. 17*, 75−86.
30. Matthew, J. B., and Richards, F. M. (1983) The pH dependence of hydrogen exchange in proteins, *J. Biol. Chem. 258*, 3039−3044.

BI700999R